AD-A179 500 UNSTEADY SEPARATED FLOWS: VORTICITY AND TURBULENCE(U) 1/1
COLORADO UNIV AT BOULDER DEPT OF AEROSPACE ENGINEERING
SCIENCES M LUTTGES 06 APR 87 AFOSR-TR-87-0304
UNCLASSIFIED F49620-83-K-0009 F/G 20/4 NL

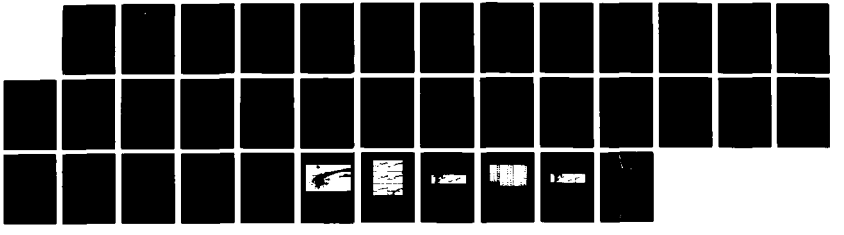

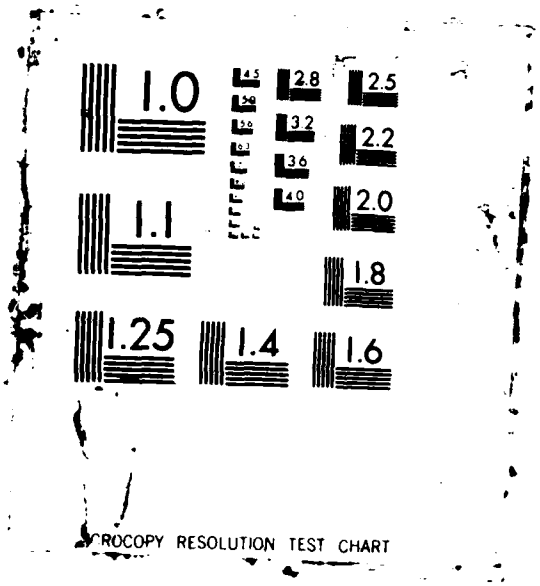
1.0
1.1
1.25
1.4
1.6
2.8
3.2
3.6
4.0
2.5
2.2
2.0
1.8
ROCOPY RESOLUTION TEST CHART

REPORT DOCUMENTATION PAGE

1a. REPORT SECURITY CLASSIFICATION: UNCLASSIFIED	1b. RESTRICTIVE MARKINGS
2a. SECURITY CLASSIFICATION AUTHORITY	3. DISTRIBUTION/AVAILABILITY OF REPORT: APPROVED FOR PUBLIC RELEASE DISTRIBUTION IS UNLIMITED
2b. DECLASSIFICATION/DOWNGRADING SCHEDULE	
4. PERFORMING ORGANIZATION REPORT NUMBER(S)	5. MONITORING ORGANIZATION REPORT NUMBER(S): AFOSR-TR- 87-0384
6a. NAME OF PERFORMING ORGANIZATION: UNIVERSITY OF COLORADO	6b. OFFICE SYMBOL (If applicable):
6c. ADDRESS (City, State and ZIP Code): AEROSPACE ENGINEERING SCIENCES, UNIVERSITY OF COLORADO, BOULDER CO 80309	7a. NAME OF MONITORING ORGANIZATION: AFOSR/NA
	7b. ADDRESS (City, State and ZIP Code): BUILDING 410, BOLLING AFB, DC 20332-6448
8a. NAME OF FUNDING/SPONSORING ~~ORGANIZATION~~ AFOSR/NA	8b. OFFICE SYMBOL (If applicable): NA
	9. PROCUREMENT INSTRUMENT IDENTIFICATION NUMBER: F49620-83-K-0009
8c. ADDRESS (City, State and ZIP Code): BUILDING 410, BOLLING AFB, DC 20332-6448	10. SOURCE OF FUNDING NOS.

PROGRAM ELEMENT NO	PROJECT NO.	TASK NO.	WORK UNIT NO.
~~2307~~ 61102F	~~A2~~ 2307	A2	

11. TITLE (Include Security Classification): (U) UNSTEADY SEPARATED FLOWS: ~~VORTICITY AND TURBULENCE~~

12. PERSONAL AUTHOR(S): M. LUTTGES

13a. TYPE OF REPORT	13b. TIME COVERED	14. DATE OF REPORT (Yr., Mo., Day)	15. PAGE COUNT
FINAL REPORT	FROM _____ TO _____	4/6/87	34

16. SUPPLEMENTARY NOTATION

17. COSATI CODES		
FIELD	GROUP	SUB GR

18. SUBJECT TERMS (Continue on reverse if necessary and identify by block number): UNSTEADY FLOWS; SEPARATED FLOWS; DYNAMIC STALL; Vortex shedding.

19. ABSTRACT (Continue on reverse if necessary and identify by block number)

Thoughout a wide combination of initial pitch angles, pitch amplitudes and pitch rates, for an NACA 0015 airfoil section, several unsteady flow initiation and development trends have been documented. The effects of mean angle of attack and reduced frequency, and the interactions between them, are generally linear (for the ranges studied). Incremental changes in reduced frequency and mean pitch angle resulted in later or earlier vortex initiation, respectively, within the pitch cycle. Other notable features of the flowfield development include the initiation of a prominent trailing edge vortex as the leading edge vortex sheds, and the convection velocity of the leading edge vortex. Similar tests employing a flat plate produced somwhat different results. The vortices were more coherent and convected at higher velocities. In general, however, the developmental trends across the parameters tested followed those of the airfoil model. Keywords:

20. DISTRIBUTION/AVAILABILITY OF ABSTRACT	21. ABSTRACT SECURITY CLASSIFICATION
UNCLASSIFIED/UNLIMITED ☒ SAME AS RPT ☐ DTIC USERS ☐	UNCLASSIFIED

22a. NAME OF RESPONSIBLE INDIVIDUAL	22b. TELEPHONE NUMBER (Include Area Code)	22c. OFFICE SYMBOL
HENRY E HELIN, CAPTAIN, USAF	202-767-4935	AFOSR/NA

DD FORM 1473, 83 APR EDITION OF 1 JAN 73 IS OBSOLETE. UNCLASSIFIED

Summary

Motion Forcing of Flow Field Structures AFOSR-TR- 87-0384

Throughout a wide combination of α_m, α_ω and reduced frequencies using a NACA 0015 airfoil, several initiation factor trends are particularly notable. The effects of α_m, reduced frequency and interactions between the two are generally linear ($r^2 > 0.90$, significant at $p<0.5$). Every 0.2 increase of the reduced frequency parameter (K) delays vortex initiation about 7% further into the oscillatory cycle. This delay factor is constant regardless of whether or not the remaining, post-initiation cycle consists of upstroke or downstroke pitching angles. The delay factor is also constant across a wide range of mean α's around which the oscillation occurs. The effect of increasing α_m is similarly well-behaved and largely independent of other factors. Every five degree increase in α_m results in the appearance of a vortex over the leading edge 10% earlier in the oscillatory cycle (cf., Fig. 01).

The appearance of a trailing edge vortex as a major unsteady flow field occurrence is similarly dependent upon α_m and reduced frequency parameter. As was the case for the unsteady separation vortex developed about the leading edge, increases in α_m values lead to the earlier appearance of the trailing edge vortex during an oscillation cycle. Also, increases in the reduced frequency parameter delay the occurrence of the trailing edge vortex in the oscillatory cycle. Increasing the reduced frequency parameter by 0.2 results in a 12% delay in the appearance of the trailing edge vortex in the oscillation cycle; the trailing edge vortex development is more sensitive to altered reduced frequency than the leading edge vortex. However, every 5° increase in α_m results in a 4.5% earlier appearance of the trailing edge vortex in the oscillation cycle; an advance in initiation approximately one-half that experienced by the leading edge vortex.

Comparatively, then, the reduced frequency induced delays are larger for the trailing edge vortex while the α_m induced advances are larger for the leading edge vortex. The added consideration of α_ω values, as cited above, indicates that a 1° increase in pitching motion amplitude produces roughly a 1% cycle delay in leading edge vortex appearance. But, this relation is absent in tests where α_m <15° and is exaggeraged where reduced frequency parameters value are 0.4 or smaller. Trailing edge vortex dependency upon α_ω is even less well behaved. These relations remain to be more fully elucidated for tests using airfoils.

Only one test parameter reliably influences the convecting velocity or traversing velocity of the leading edge vortex over the airfoil surface. Neither α_m nor α_ω alter this velocity in a simple, reliable manner. However, larger reduced frequency values produce increases in the relative convecting velocity, V/V_∞. This relation depends upon whether the vortex was initiated before or after maximum angle of attack (α_{max}) was attained in the oscillation cycle (Fig. 02). For initiation prior to α_{max}, the average convecting velocity was V/V_∞ =0.310. For initiation after α_{max}, the average velocity was V/V_∞ =0.137. Within each of these two conditions a positive relation between K and V/V_∞ holds such that linear regression yields r^2>0.95.

Using the same evaluations of V/V_∞ in tests of a flat plate, the results are somewhat different. A vortex initiated before α_{max} is obtained in the oscillation cycle yielded convection velocities not unlike those recorded for a NACA 0015 airfoil under similar conditions. However, vortices initiated after α_{max} in the oscillation cycle exhibited quite high convection velocities unlike those recorded for the airfoil (cf. Fig. 02). Without speculating about the particular meaning of these observations, it is clear that different lifting surface geometries can have a dramatic effect on convecting velocities of the elicited vortices. As pointed out

below, the geometry change appeared to have little consequence for vortex initiation.

That the above trends in observed initiation of flow field structures (cf. Fig. 03 and Fig. 04) are robust and fairly general has been shown through our tests based upon harmonic oscillations of a flat plate. Under these test conditions, the leading edge vortex initiation occurred earlier in the oscillation cycle with increases in α_m. In fact, every 5° increase in flat plate α_m resulted in a 6.25% advance in the cycle where the leading edge vortex was initiated; a value close to that measured using the NACA 0015 airfoil. Every 0.2 increase in reduced frequency delayed the leading edge vortex by approximately 10% of the oscillation cycle; a value between 7% and 12% values seen for the leading and trailing edge vortices, respectively, using the symmetric airfoil.

What the above investigations show is that certain distinct flow field properties (e.g., vortex initiation, V/V_∞), elicited by driven lifting surface motions, are quite predictable within certain parameter ranges. To date, other flow field characteristics (circulation velocities, vorticity) remain to be determined. Indeed, some of the effects of certain motion parameters apparently are quite complex. Overall, however, the fact that major separation structures in the flow field are related linearly and independently to unsteady driving mechanisms suggests that many other characteristics of the flow field must be similarly well behaved, albeit complex.

Characterization of Flow Field Structures

Despite the predictable appearance of flow field structures related to lifting surface motions there are no a priori conclusions to be made regarding the uniformity or identity of such structures. Also, the strength and nature of interactions between the flow structures and the

adjacent lifting surface remain to be determined. Only fragmentary results have been collected, to date, on these crucial characteristics of the emerging flow field structures.

A series of single wire, hot wire anemometry measures have been made in conjunction with flow field visualization. The anemometric measures, using a single wire, yield velocity profiles for the observed flow field disturbances but are limited by the absence of complete velocity vector information. Nevertheless, the vortex structure which evolves on and passes over the lifting surface adds circulation velocities to convection velocities such that at some point in the passage of the vortex a velocity peak is recorded by the hot wire. This point in time and position about the surface must correspond to the induced tangential velocity of the vortex circulation being aligned exactly with vortex convection direction, if three-dimensional effects are ignored. This rationale had been formalized previously by Oseen (1927) and Hamel (1916) as reviewed by Schlichting (1979).

Using the above rationale, flow visualization was arranged such that the velocity peak recorded on the hot wire probe was the phase trigger for 7 sec. stroboscopic illumination. The resulting pictures reveal the instance of maximally additive velocities in the flow field. By repeating this process at a variety of distances from the airfoil surface and at different chord locations, a reproducible index of vortex size and strength is obtained. The size, of course, derives from the mean distance the hot wire probe may be displaced from the airfoil surface and still record velocity peaks significantly different from V_∞. Another way to view these data is that a time dependent, large fluctuation in the outer portions of the velocity profiles can be recorded and mapped.

The above correlations of visualization and velocity reveal the following vortex characteristics: (1) Vortex diameter increases with increased α_m up to an asymptotic value which occurs spatially at approximately 0.70 chord. (2) Vortex diameter is unaltered by variations in α_ω. (3) Vortex diameter is asymptotically and inversely related to increases in reduced frequency. (4) Increases in α_m decrease peak V/V$_\infty$ values at the time a vortex is present. (5) Larger α_ω values increase V/V$_\infty$ peaks modestly (<20%). (6) Increases in reduced frequency increase V/V$_\infty$ asymptotically up to velocities of 2.5 V$_\infty$ when a vortex is present. If the diameter and velocity information is combined, it suggests that the more energetic the driving of unsteady flow field structures, the more likely that both vortex size and circulation will increase over the chord while convecting downstream. In less energetic driving conditions, the vortex size-velocity product attains a maximum value before the full chord is traversed. And, under the least energetic conditions tested, the vortex circulation-size product attains a maximum value over forward chord positions, then the vortex departs from the airfoil surface before reaching the trailing edge. In the latter two conditions, flow visualization suggests the presence of cataclysmic flow separation during some portion of the oscillation cycle.

Three-Dimensionality of Unsteady Separated Flows

The three-dimensional flow structures elicited by unsteady separated flow conditions remain largely a matter of speculation. Systematic research on this interesting problem has not been pursued except for that recently reported at the III International Flow Visualization Conference (Adler et al., 1983). The problem can be broadly subdivided into two obvious components: (1) the three-dimensionality of flow fields elicited by a two-dimensional test situation and (2) the three-dimensionality of

flow fields in a three-dimensional test situation. The former type of condition has been cited often in rather spurious informal fashion. The latter test situation surely influences the nature of unsteady separated flow fields about swept and delta wings as recently noted by Gad-el-Hak (1983) and by Carta (1983). A great amount of work remains to be done in this area.

The simple three-dimensional model we have used to initiate the three-dimensional study of unsteady flows is a symmetric airfoil (NACA 0015) section fitted with a wing tip exhibiting a radius of curvature consistent with the airfoil thickness. Some typical results are provided in Fig. 05. First, using a reduced frequency of approximately 1.0 (an oscillation cycle of approximately 100 msec in duration) two α_m values were used with an α of 10°. For the dashed and solid lines, respectively, α_m = 15° and 12°. The Re number was 60,000 for these tests.

As might be expected from the previous discussion, the convection velocities for the leading edge vortex were higher for α_m = 12° than for α_m = 15°. The presence of a wing tip and associated wing tip vorticity did not alter convection velocities or the α_m effect on these velocities. The velocities were similar to those seen in two-dimensional tests. Similarly, the leading edge vortex formed at the point in the oscillation cycle predicted from earlier work. In Fig. 06, the test conditions are examined using just one simple index of the altered three-dimensionality of the flow. Beginning at t = 0 the airfoil was at the maximum angle of attack, 2 . Approximately 75% of the cycle later, the leading edge vortex shed into the wake. Throughout the whole oscillatory cycle, the spanwise locations of smoke lines both passing over and passing under the airfoil were noted. What is plotted is the displacement of those smokelines in the spanwise direction as the lines pass the trailing edge as a function of

time. Significant three-dimensionality is produced in the flow field; this three-dimensionality is time-dependent. The three-dimensionality indicated by smokeline displacements spanwise is phase coincident with the two-dimensionally prominent vortex center of the passing leading edge vortex. The later, smaller peak of three-dimensional displacement is coincident with the appearance of the trailing edge vortex. Interestingly, the latter, counter-rotating vortex provided a three-dimensionality of the same sign as the passing leading edge vortex.

As a plane of smokelines is moved out to the wing tip, the three-dimensionality of the wing tip vortex is encountered. The oscillation of the wing both increases and decreases wing tip vorticity. This well-known effect of angle of attack is appropriately realized as more or less tightly rolled vortices, respectively. The details of this flow are cited elsewhere (Adler et al., 1983) as an example of an inherently three-dimensional structure acted upon by unsteady separation. When the plane of smokelines is moved systematically from wing tip to inboard positions, the transition from tip to leading edge vortex dominated flow is encountered. In these instances, the interaction between two, three-dimensional flows may be examined.

The relation of three-dimensionality in flow field structures to underlying unsteady flow parameters is unclear. However, we have demonstrated that the inherent complexity of such flows is well behaved and amenable to detailed, multiple exposure flow visualization analyses. Such analyses are being continued. A digitizing pad is used to record the flow structures as quantitative files for possible three-dimensional reconstructions using computer graphics.

Thus, the three-dimensional character of unsteady separated flows can be examined for the temporal and spatial responses elicited by a variety of lifting surface motions.

Dragonfly Lift Generation

Comparisons between the Weis-Fogh mechanism (Weis-Fogh, 1973) of lift generation and the dragonfly mechanisms of lift generation (Luttges et al., 1983) reveal the existence of very different means for exploiting unsteady flows. Both mechanisms appear to involve vortex generation and utilization but here the similarities stop. Some of the differences are cited below. A broad question of some considerable significance is obvious: Do unsteady flows foster a wide variety of quite different lift generation mechanisms?

According to Lighthill's analyses (1973, 1975) of the Weis-Fogh mechanism based upon two-dimensional, inviscid flow theory, the "fling" process evokes a flow with an instantaneous angular velocity sufficient to provide high lift values in the absence of vortex shedding. The "fling" dynamics follow the clapping together of the wings and arise from the parting of the leading edges of the wings. The trailing edges of the wings remain closed. Thus, "starting vortices" dominate the flow briefly and there is no need to consider shedding into the virtual wake. The symmetry of these flow structures yield an upward force which is surprisingly continuous as the wings show increasingly large, effective angles of attack.

When convection and diffusion terms were added by Lighthill to his analysis (1975), the fluid "memory" of viscous effects became an important determinant in the lift generation mechanism. A net flow derives from the sink created during the fling as well as from the convective-enhanced flows originating beneath the wings. The "starting flow" characteristics associated with a 400 Hz wing beat largely prevent the development of reversed flow and stall. And, instances of reversed flow are generally packaged in a leading edge bubble such that full separation does not develop behind the bubble. In fact, the compliant wing structure might be

expected to conform to the resulting pressure gradients and to effectively exhibit a desirable increase in camber which retards separation. Not surprisingly, maximum lift in the Weis-Fogh experiments with the wasp, Encarsia formosa, arise just as the fling begins to pull apart the wings at the trailing edges. Lighthill speculates that at this point in the wing beat cycle, diffusive forces tend to decrease the undesirable effects of shedding vorticity and counter-rotating vortices.

At the end of the wasp wing beat cycle (approximately 130° arc) the "flip" occurs. The instantaneous change in angle of attack intercepts existing vortex-associated flow such that the effective angle of attack remains modest. The weak "starting vorticity" does not disrupt the flow memory initially produced and energized by the clap and fling. Thus, only one maximum lift episode occurs during each wing beat cycle. Nevertheless, continued positive lift is hypothesized by Lighthill to occur throughout the wing beat cycle; an idea not substantiated by Weis-Fogh's observations (1973).

Some crucial facts should be noted in regard to the Weis-Fogh mechanism before turning to comparisons with our observations on the dragonfly. First, the overall lift of the wasp as a model of the Weis-Fogh mechanism yields C_L values of approximately 3.0. Secondly, the flow structure interacts about the whole wasp such that a single large flow structure (approximately two times the largest dimension of the wasp) immerses this insect (Maxworthy, 1979). Thirdly, the wing-body orientation is such that wings beat through a horizontal path during hovering and, fourthly, the wings beat at a high frequency while clapping together at the end of each stroke.

In contrast, the dragonfly remains horizontal during hovering and fast

forward flight. The wings move through vertical planes at an order of magnitude less frequency (approx. 20 - 40 Hz) and without clapping. Norberg (1975) Weis-Fogh (1973) and Somps (1982) estimate C_L values of 5.0 or more across a range of assumptions and calculations (for example, the estimated Re numbers for the wasp are an order of magnitude smaller than those of the dragonfly). The flow visualized for tethered dragonfly flight episodes indicates the presence of multiple, reliable vortices with chord length dimensions rather than the relatively large dimensions observed in the moth. Whereas the elicited flow envelops the whole wasp, the flow elicited by the dragonfly wings is local to each lateral pair of wings. The stroke arc of the dragonfly wing is approximately 80^{o} while that of the wasp is at least 130^{o}. And finally, the geometric angles of attack of the dragonfly wing appear much more exaggerated than those of the wasp wing.

What do each of these contrasts indicate? Overall, these two insects have probably evolved very different means for exploiting unsteady flows. A "starting vortex" in the case of the dragonfly cannot depend upon a void or "sink" such as that elicited in the parting of wings during the "fling" in the wasp. The dragonfly wings remain at 90^{o} angles from each other at the top and bottom of the stroke cycle. A simplified inviscid model of lift production would not suffice for explaining dragonfly lift generation as it does in explaining lift generation achieved by a Weis-Fogh mechanism (Lighthill, 1973). Convective effects might be crucial to the flow-wing interactions in the dragonfly. And, the results of shedding vorticity actually may be utilized by the dragonfly.

Unlike the continuous, compliant single (latched tandem wings) wings of the wasp which has a small aspect ratio, the dragonfly has two separate tandem wings of considerably higher aspect ratio and of potentially different phase dynamics. Thus, since the rapid shedding of elicited

vortices may not be avoidable, a mechanism may exist to exploit these shed vortices; a phase-variable, nearby lifting surface, a second wing. Such a hypothesized interaction between front and back wings is consistent with both the size scale and the visualized circulation of elicited vortices. In addition, this supposed interaction between tandem wings would generate lateralized lift characteristics consistent with the roll instabilities sometimes seen in the free flight of dragonflies and would be consistent with the brief, high lift episodes demonstrable in each complete wing stroke cycle (contrasted with the somewhat more continuous lift generated for the Weis-Fogh mechanism). Recent flow visualization records, collected in our laboratories this summer (Fig. 07), show the small reproducible vortices elicited around a single dragonfly wing. The shedding of these vortices is obvious as well as the serial arrangement of rotating and counter-rotating vortices. These flow structures are clearly different in size and circulation from those postulated by Weis-Fogh (1973) and simulated physically by Maxworthy (1979). Some of these differences have been cited earlier by Savage et al. (1979) who favors a hypothesized use of small, surface entrapped vortices.

Since the dynamics and analyses of the Weis-Fogh lift generation mechanism apparently are not the same as dragonfly lift generation mechanisms, the latter requires a considerable amount of additional research effort. Much of the needed effort already has been expended in collecting raw data from the dragonfly. The approach which has been taken to date will be outlined below. The analyses and data reduction focuses are similarly summarized.

A "model" of dragonfly wing and flow interactions. To simplify the characterization of wing-flow interactions, a unique testing situation has

been arranged. Dragonflies caught on the day of testing are tethered by cyanoacrylic cement to a long, thin rod instrumented with a strain element. A surgical incision is made in the thoracic sclera next to the cement point to permit the insertion of fine stainless steel electrodes. These electrodes are positioned about the thoracic ganglion such that small, brief electrical pulses directly elicit wing motion. By altering voltage levels, pulse duration and pulse frequency, it is possible to elicit comprehensive wing stroke cycles which are complete in terms of both full stroke arcs ($\leq 100^{o}$) and associated angles of attack. Threshold levels of stimulation produce front wing flight activity and suprathreshold levels produce appropriately phase-related recruitment of hindwing flight activity. The net effect of this arrangement is to electrically "drive" wing motion in sustained, stereotyped fashion. In doing so it is possible to study, in elaborate detail, wing-fluid interactions and lift generation.

The creation of a "model" dragonfly using the existing dragonfly geometry, hardware and controls is unique. Thus, questions may arise regarding the adequacy of this preparation in understanding normal dragonfly flight. To date our only answers to such questions are based upon photographs of free flight wing motions, tethered dragonfly wing motions and artificially driven wing motions. Across all these conditions, the wing motions are consistent and stereotyped. There can be little doubt that some variations in flight activity occur but such subtle variations, for the time being, reside outside the domain of an initial analysis of flight mechanisms.

The test conditions for which considerable data exist are as follows: (1) changes in angle of attack (2) with wing stroke arc angles, (3) changes in wing-flow interactions with increased stroke frequency and arc angle, (4) changes in lift generation with increased stroke frequency and arc

angle.

During these tests, it became obvious that the wing-flow interactions were extremely complex. To simplify the tests even further, flight motions were elicited from a dragonfly with a single wing (all others having been removed). As may be seen in Fig. 08, a single wing elicits rather pronounced, complex local vortical structures. Again, the rotating vortical structures exhibit primary, secondary, and even tertiary counter-rotations.

Given the raw data currently available, it should be possible to determine the manner in which vorticity arises in the fluid adjacent to the wing and to estimate the relative strength of such vorticity. The temporal and spatial features of the resulting vortices can be similarly related to wing-flow interactions. And finally, these dynamics can be subdivided into generation versus utilization phases. The mechanisms and energy related to producing proximal vortical flow structures can be correlated with the lift (thrust) obtainable from such vortical structures. These analyses, based upon flow visualizations, wing dynamics and simultaneous lift measurements, will build in complexity from the single wing model through the double tandem wing model and then through the intact dragonfly model. Aiding in these analyses will be the high-speed video tapes (2000 frames/sec; high pixel density) prepared by a demonstration team from Spin Physics (Kodak) and the more detailed force measurements obtained from the recently revised, sensitive force balance.

What Can We Learn?

First, we are in the position to document use of unsteady separated flows by insects to produce very high lift coefficients. At this point, the Weis-Fogh mechanism has not enjoyed direct experimental verification

such as that we are developing for the dragonfly. More importantly, the dragonfly lift generation mechanism appears very different from the hypothesized Weis-Fogh mechanism. This seems to indicate that a variety of unsteady separated flow mechanisms, a general class, may exist for potential use in generating high lift coefficients. The Weis-Fogh mechanism and the dragonfly mechanism may be but two examples of this class of mechanism.

The extraction of effective combinations of dynamic variables ($\dot{\alpha}$, α_m, and wing beat frequency) from our studies is straightforward. But, questions may arise regarding the appropriate scaling to more realistic Re numbers. To some extent it is premature to pose this question. Nevertheless, the possible relation to boundary layer perturbations may not require significant scaling changes. Both viscosity and effective Re number values may fall into the germane range (cf., Sears and Telionis, 1975) if considered to be novel boundary layer control devices. To be sure, the discovery of a whole new class of lift augmentation mechanisms produces many more questions than answers.

The long-term goals of the insect studies is to demonstrate and elucidate the effective uses of unsteady flows. To this end, quantification of initiation factors, sustaining factors and utilization factors will be carried out to the largest extent possible. The consideration of the importance of the three-dimensional characteristics of the system must be fostered by appropriate measures. Using these data, appropriate dimensional analyses and similitude arguments can lead to new insights into the use of unsteady flows about lifting surfaces.

(a) description of work achieved in accelerated flow.

In our investigations thus far, we placed an NACA 0015 airfoil into a flow of nearly constant acceleration, starting from rest. A low turbulence wind tunnel with a 3 ft by 3 ft test section was redesigned for this purpose (in cooperation with our able technician Mr. W. Bank).

Investigation at this stage is mainly by flow visualization which has proven uniquely suited to bring out the basic separation phenomena. Fig. 09 shows some basic modes of visualization used thus far and introduces some of the nomenclature and the characteristic Reynolds number relevant for these experiments. (This poster was one of five winners among ca. 90 entries at the APS-Fluid Dynamics Division Meeting, Nov. 83). Thus far we have completed visualization of the angle of attack dependence of unsteady separation at a fixed Reynolds number R = 5200 (Freymuth et al., 1983 a, b, c, d).

Let us briefly describe some of the separation phenomena and their dependence of flow parameters as already observed by us. At intermediate Reynolds numbers (R of order 5000) after flow startup, a boundary layer develops over the airfoil which then begins to thicken near the leading edge of the suction side. Such a protrusion evolves quickly into a vorticity separation tongue which develops into a primary vortex which then induces a secondary separation tongue to the left of it with the consequence of additional vortex development. An example is shown in the middle sequence of Fig.10 for an angle of attack $\alpha = 20°$. The highly ornamental vortex pattern development finally gets blurred by the onset of turbulence. Unfortunately, theoretical development lags far behind, only the initial development of the first vortex tongue has been calculated (Mehta and Lavan, 1975), secondary and higher order vortices await future theoretical investigation. After the onset of turbulence, a turbulent large scale structure sheds into the wake and interacts with the trailing edge vorticity which separates quickly after flow startup. A more detailed description is given by Freymuth et al. (1983). At high angles of attack ($\alpha \geq 40°$) there is an intermediate stage between laminar vortices and the onset of turbulence where small vortices form vortex groups prior to turbulent decay as shown for instance in Fig.09. The final stage of the

separation process is an unsteady turbulent vortex street shed from the leading and trailing edges of the airfoil.

It should be mentioned that even at angles of attack below the static stall angle separation does not completely cease. Rather, separation moves more toward the trailing edge of the airfoil, i.e. with decreasing angle the area over the airfoil for which the flow remains attached increases (Freymuth et al.,1983), but not abruptly.

We are in the process of obtaining the Reynolds number dependence of separation phenomena. Fig. 10 shows results at an angle of attack $\alpha = 20°$. Laminar separation is dominant in the vortex initiation of accelerating flow around airfoils up to modest Reynolds numbers (up to R = 6000). It continues to dominate the later development of vortices at low Reynolds number over a considerable time. In contrast, at high Reynolds numbers (R=52400) laminar separation initiates the development of an attached turbulent boundary layer from several nearly simultaneously occurring separation tongues, i.e., laminar separation initiates transition to turbulence. Finally, however, the turbulent boundary layer separates and the leading edge separation forms a turbulent vortex which sheds into the wake. This process is at present intensely investigated and probably sheds light on other high Reynolds number separating flows.

Finally we did some minor investigation into the effect of geometry on unsteady separation (Freymuth, et al., 1983) by considering accelerated flow around a flat plate, a round plate, a circular cylinder and a sphere. The main result thus far is that dependence on geometry is not dramatic, except for sharp-edged bodies versus round edged bodies at small angles of attack.

Theoretical Studies

The purpose of our theoretical studies is to further our understanding of vortical and unsteady flows through analytical and numerical approaches. These studies are not unrelated to the works of the experimental counterpart in our research group; numerical modeling is intended to simulate some experiments in the laboratory. In addition, some theoretical discoveries may suggest new directions to the experimentalists.

After three years' support of the Air Force Office of Scientific Research, we have become familiar with the literature published on the concerned subjects, learned basic analytical and numerical techniques for solving vortical and unsteady flow problems, and produced five papers that were published in technical journals or presented in professional meetings. First, we will provide a general review of the work that has been completed so far.

I. Review of the Theoretical Studies

Our work can be grouped roughly into the following two general categories:

(1) Study of the interaction between airfoil and discrete vortices.

This study is divided into two parts depending on whether the vortices are stationary or moving relative to the airfoil. Vortex initiation or generation conditions are best left, for the time being, to experimental determinations. Concerning a stationary vortex above a flat-plate airfoil, Saffman and Sheffield (1977) found that lift of an airfoil can be increased by a captured vortex. Unlike the leading edge flap suggested by Rossow (1978), this lift augmentation technique has the advantage that it does not require any change in airfoil shape and, therefore, can avoid the

tremendous increase in form drag. The investigation has been extended by us to include the effects of airfoil thickness and camber on vortex stability and augmented lift (Huang and Chow, 1982). However, in a later work (Chow and Huang, 1983) we discovered numerically that all of the equilibrium positions of the vortex that are found to be stable by the previous small perturbation analysis become unstable when the vortex is displaced with a finite amplitude. Interaction between an airfoil and vortices moving relative to it has been a problem encountered mainly by engineers working on helicopter blade design and performance calculations. Considering the influence on lift, we have made an inviscid analysis of the flow past an airfoil in whose proximity there is a moving vortex which is either a free vortex coming from a far-away location or a captured vortex disturbed from its equilibrium position (Chow and Huang, 1983).

It is found that the vortex can increase or decrease the lift depending on its position and the attitude of its motion. The result for an approaching vortex is generally in agreement with that obtained by Wu, Sankar, and Hsu (1983) from viscous flow computation and with that obtained by Caradonna, Desopper, and Tung (1982) using a transonic flow code while assuming that the vortex path is not influenced by the airfoil. To explain exactly how a moving vortex can generate an unsteady lift or diminish it remains a part of our continuing research effort.

In addition to the interaction with a single vortex, we have also studied the interaction of airfoil with a train of vortices. These vortices are used to simulate those generated intermittently by an oscillating spoiler or a rotating cam installed on the upper surface of an airfoil, corresponding to the experimental arrangements of Francis et al. (1979), Robinson and Luttges (1983), and Viets et al. (1979), respectively.

Our results (Chow and Chiu, 1983) based on numerical computations show that after vortices are released at a fixed frequency from a given position above an airfoil, lift increases with time in an oscillatory fashion. The mean lift averaged over one cycle increases continuously and approaches an asymptotic value. This asymptotic lift increases with the frequency at which vortices are released. It is also found that this lift augmentation technique is more efficient at higher angles of attack of the airfoil, a condition also recently observed in our experimental studies (Luttges, personal communication).

(2) Study of wakes and boundary layers around bodies in unsteady motion

A large number of papers have been published in this area. Recent literature surveys can be found in the book by Telionis (1981), and in the review paper by McCroskey (1982) particularly for dynamic stall of airfoils.

Our research on this subject started with the examination of the initial behavior of the flow in close proximity to an impulsively started body. The study of the wake shed by an airfoil (Chow and Huang, 1983) leads to the conclusion that both the initial lift and drag of a cusped airfoil are increased either by increasing camber and angle of attack or by decreasing the thickness. For an airfoil of finite trailing-edge angle, however, both lift and drag vanish at the initial instant. This provides an explanation of the discrepancies shown in numerical results published by different authors on the initial behavior of impulsively started airfoils. The method of apparent mass used in this paper is also applied to compute the lift and side forces on an aircraft fuselage where cross sections are isosceles triangles or are of the shape formed by two circles (Huang and Chow, 1983). On the other hand, the method of matched asymptotic

expansions is adopted to study the boundary layer development on an elliptic cylinder impulsively set into translational and rotational motion (Billings and Chow, 1983). It is found that pitch-up rotation accompanying translation at an angle of attack is capable of preventing the early formation of a leading edge separation bubble.

Project Bibliography

Robinson, M.C. and Luttges, M.W., "Unsteady Flow Separation and Attachment Induced by Pitching Airfoils," AIAA 21st Aerospace Sciences Meeting, AIAA Paper AIAA-83-0131, Jan. 1983, pp. 1-14.

Adler, A.N., Robinson, M.C., Luttges, M.W., and Kennedy, D.A., "Visualizing Unsteady Separated Flows," Third International Symposium on Flow Visualization - University of Michigan, Ann Arbor, Michigan, Sept. 1983, pp. 806-811.

Robinson, M.C. and Luttges, M.W., "Unsteady Separated Flow: Forced and Common Vorticity about Oscillating Airfoils," Workshop on Unsteady Separated Flow, United States Air Force Academy, Aug. 1983, pp. 83-89.

Robinson, M.C. and Luttges, M.W., "Vortex Generation Induced by Oscillating Airfoils: Maximizing Flow Attachment," Eighth Biennial Symposium on Turbulence, University of Missorui, Rolla, Sept. 1983, pp. 1-10.

Luttges, M.W., Somps, C., Kliss, M. and Robinson, M.C., "Unsteady Separated Flows: Generation and Use by Insects," Workshop on Unsteady Separated Flow, United States Air Force Academy, Aug. 1983, pp. 93-97.

Kennedy, D.A., "Aerodynamic Agility Resulting from Energetic Separated Flows. Workshop on Unsteady Separated Flows, United States Air Force Academy, Aug. 1983, p. 29.

Freymuth, P., Bank, W., and Palmer, M., "Use of Titanium Tetrachloride for Visualization of Accelerating Flow Around Airfoils," Third International Symposium on Flow Visualization, Sept. 6-9, Ann Arbor, Michigan, Proceedings, Vol. III, pp. 800-805.

Freymuth, P., Bank, W., and Palmer, M., "Visualization of Accelerating Flow Around an Airfoil at Angles of Attack 0^{o}-30^{o}", 8th Biennial Symposium on Turbulence, Rolla, Mo., Sept. 26-28

Freymuth, P., Bank, W., and Palmer, M., "Comparative Visualization of Accelerating Flows around Various Bodies, Starting from Rest," Workshop on Unsteady Separated Flow, Aug. 10-11, U.S. Air Force Academy, Colorado Springs, Colorado, Proceedings, 1983, pp. 41-46.

Freymuth, P., Bank, W., and Palmer, M., "Visualization of Accelerating Flow Around an Airfoil at High Angles of Attack," Accepted for publication in Zeitschrift fur Flugwissenschaften and Weltraumforscheng (ZFW), 1983.

Freymuth, P., Bank, W., and Palmer, M., "Flow Visualization and Hotwire Anemometry," Accepted for Publication in TSI Quarterly, 1983.

Billings, D.F. and Chow., C-Y., "The Unsteady Boundary Layer on an Elliptic Cylinder Following the Impulsive Onset of Translational and Rotational Motion," AIAA Paper No. 83-0128, January 1983.

Chow, C.-Y. and Huang, M.-K., "Unsteady Flows About a Joukowski Airfoil in the Presence of Moving Vortices," AIAA Paper No. 83-0129, January 1983.

Huang, M.-K. and Chow, C.-Y., "Apparent-Mass Coefficients for Isosceles Triangles and Cross Sections Formed by Two Circles," Journal of Aircraft, August 1983.

Chow, C.-Y. and Chiu, C.-S., "Unsteady Aerodynamic Loading on an Airfoil due to Vortices Released Intermittently from its Upper Surface," Workshop on Unsteady Separated Flows, United States Air Force Academy, August 1983, pp. 64-65.

Personnel Presently Involved (Fall 1983)

Faculty

M. Luttges

C. Y. Chow

D. A. Kennedy

Graduate Students

R. Leben

C. L. Chen

M. Robinson

M. Kliss

J. Adler

M. Palmer

C. Somps

N. Mossberger

Undergraduates

L. Beeman

N. Searby

R. Jones

Technical Support Staff

W. Bank

R. Meinzer

Secretarial Staff

J. Button

T. MacGregor

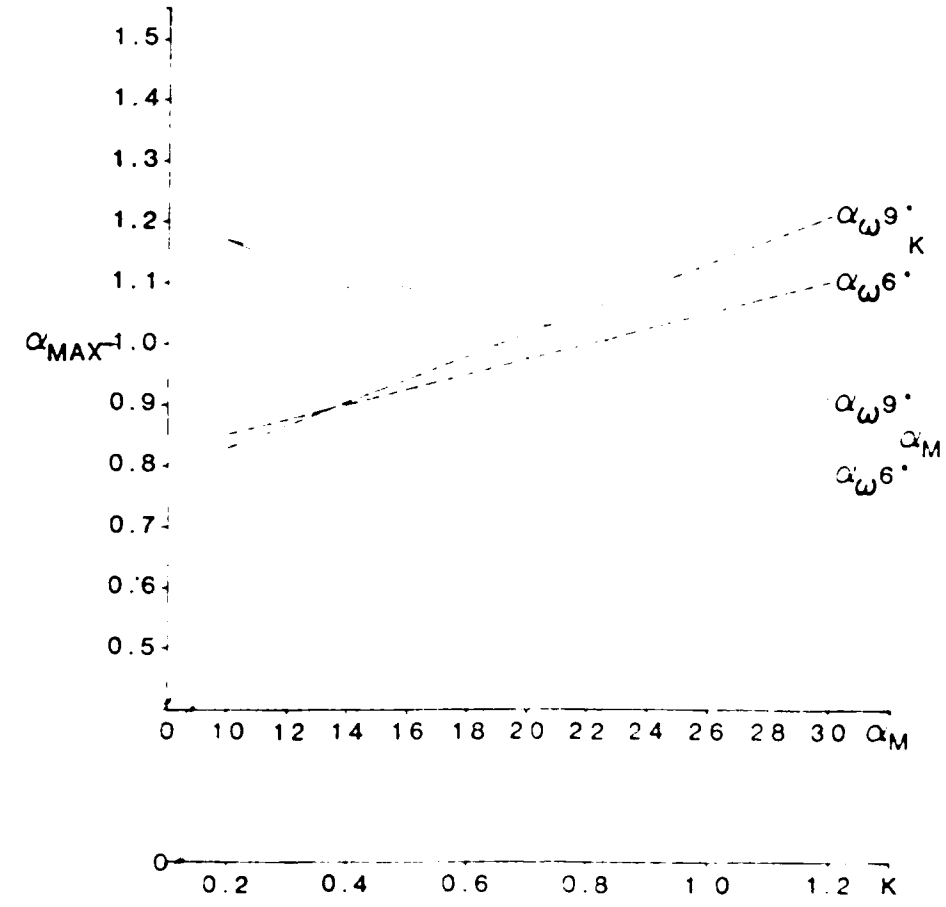

Figure 6(a. Leading edge vortex initiation in the oscillation cycle. Dependence upon reduced frequency (K) and mean oscillation angle (α_M) is shown as related to two different oscillation amplitudes, $\alpha_\omega = 6^\circ$ and $\alpha_\omega = 9^\circ$. The oscillation cycle is divided into tenths with unity representing the maximum angle of attack, α_{max}, achieved. These data show a linear fit of better than $r^2 = .95$. NACA 0015, oscillated around 0.25 chord, 6 in. chord. $Re = 60{,}000$.

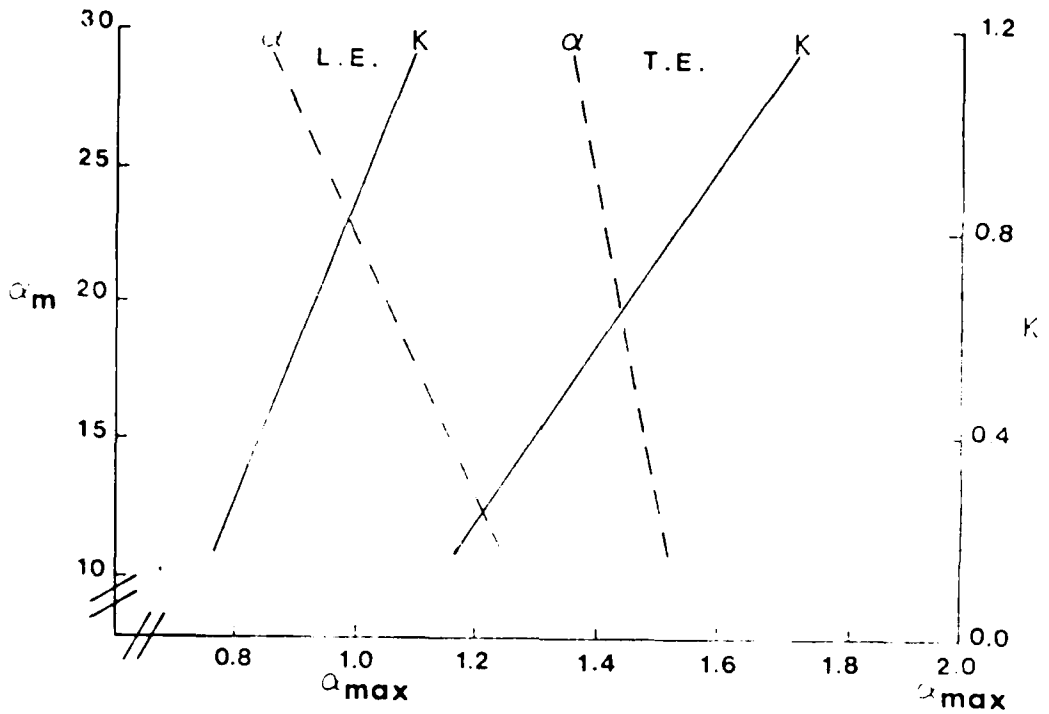

Figure 01b. Point in the sinusoidal pitching cycle when a leading edge vortex (L.E.) appeared over the 0.3 chord location or a trailing edge vortex (T.E.) appeared over the 1.0 chord location. As noted, the oscillation cycles are divided into tenths with whole integers representing α_{max} values in the cycle. The lift ordinate represents the average angle of attack, α_m, around which pitch changes occur symmetrically and the right ordinate represents the reduced frequency parameter, K, achieved in the oscillation dynamics. The linear regression fit is better than $r^2 = 0.90$ for all lines depicted. These data were obtained from flow visualization using a NACA 0015 airfoil pitching around the 0.25 chord location and having a 6 in. chord.

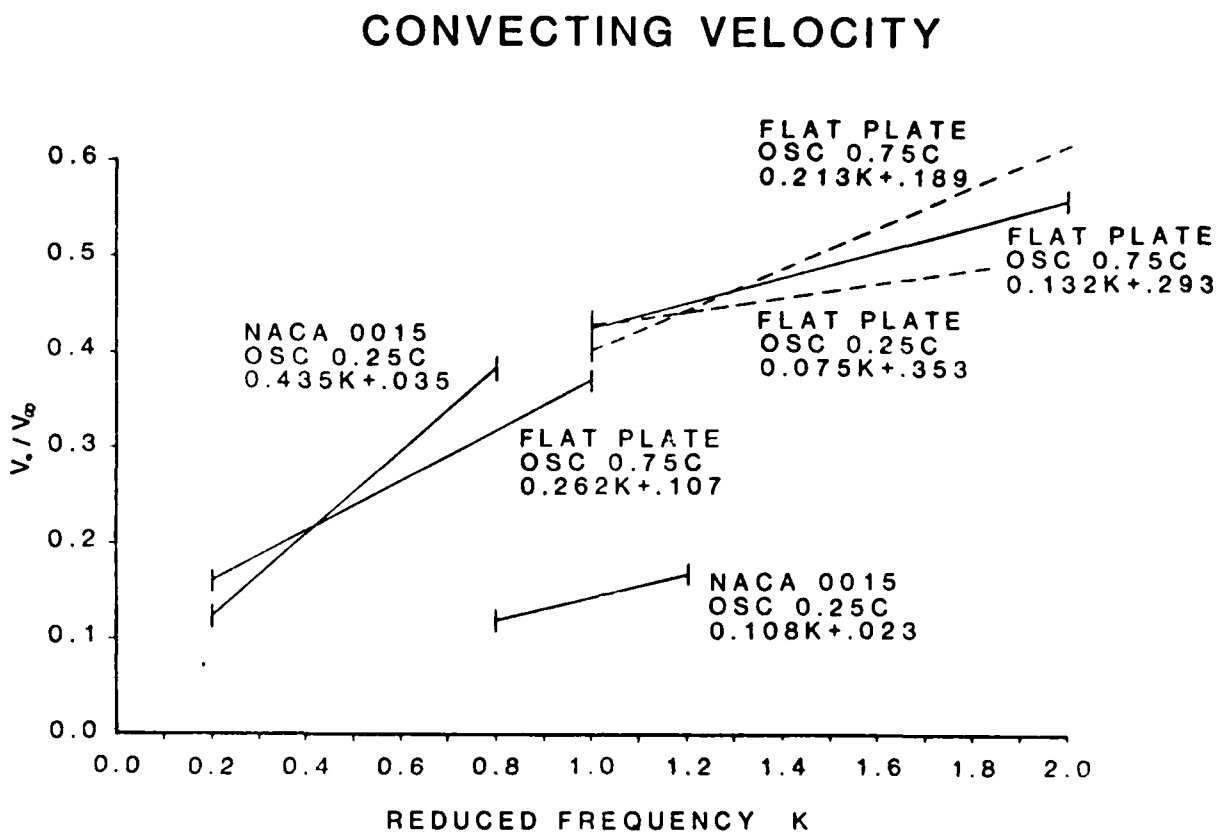

Figure 02. Convection velocities of the leading edge vortex. Determined by flow visualization where the time to pass from 0.3 to 1.0 chord was measured and determined by hot wire anemometry where the time for a velocity maximum to pass from 0.2 - 1.0 chord was measured. The least squares linear regression fit was better than $r^2 = 0.95$ in all instances depicted. Solid line data were obtained by flow visualization and dotted line by anemometry tracking of peak velocity. To maximize the linear regression fit, the data are given for low K tests where the leading edge vortex was initiated prior to α_{max} in the pitching cycle and for higher K values where the leading edge vortex was initiated after α_{max}. The slopes and intercepts are as noted. OSC indicates the pivot location around which oscillation occurred.

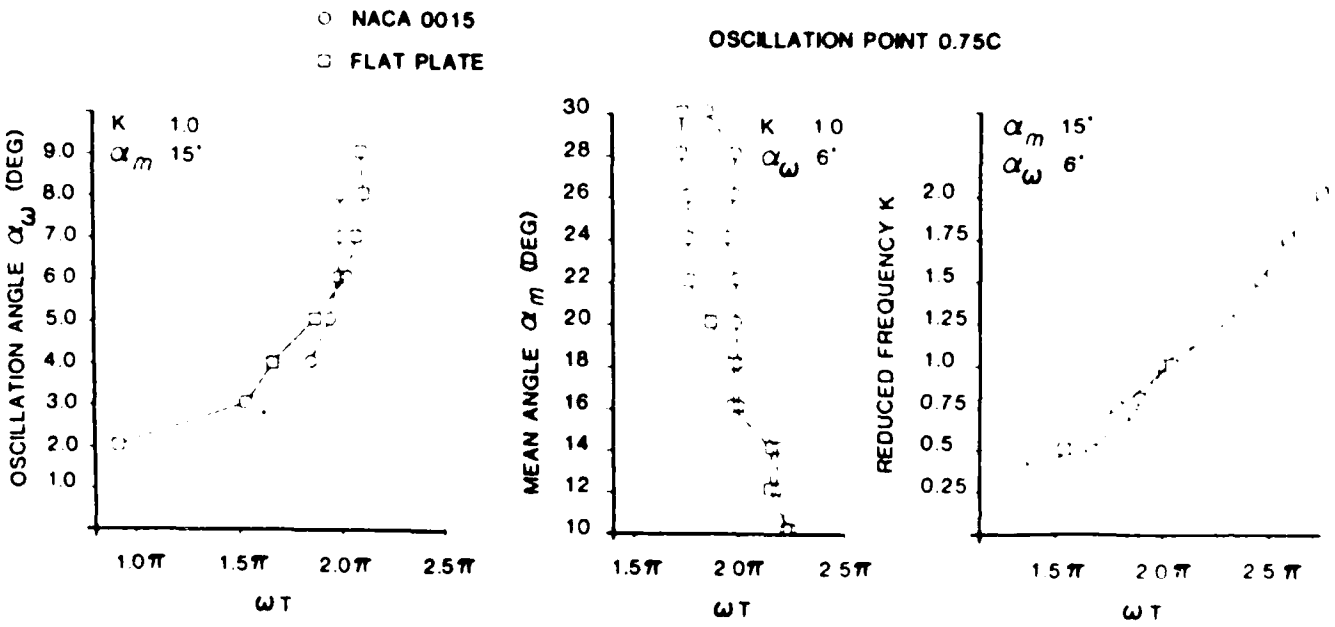

Figure 03. Comparison of α_m, [illegible] and reduced frequency parameter (K) effects on the visualized appearance of a leading edge vortex over the 0.2 chord location. The flat plate had a 10 in. chord, whereas the NACA 0015 airfoil had a 6 in. chord. Both surfaces were oscillated about the 0.75 chord location. Re number for all tests was ≈ 50,000.

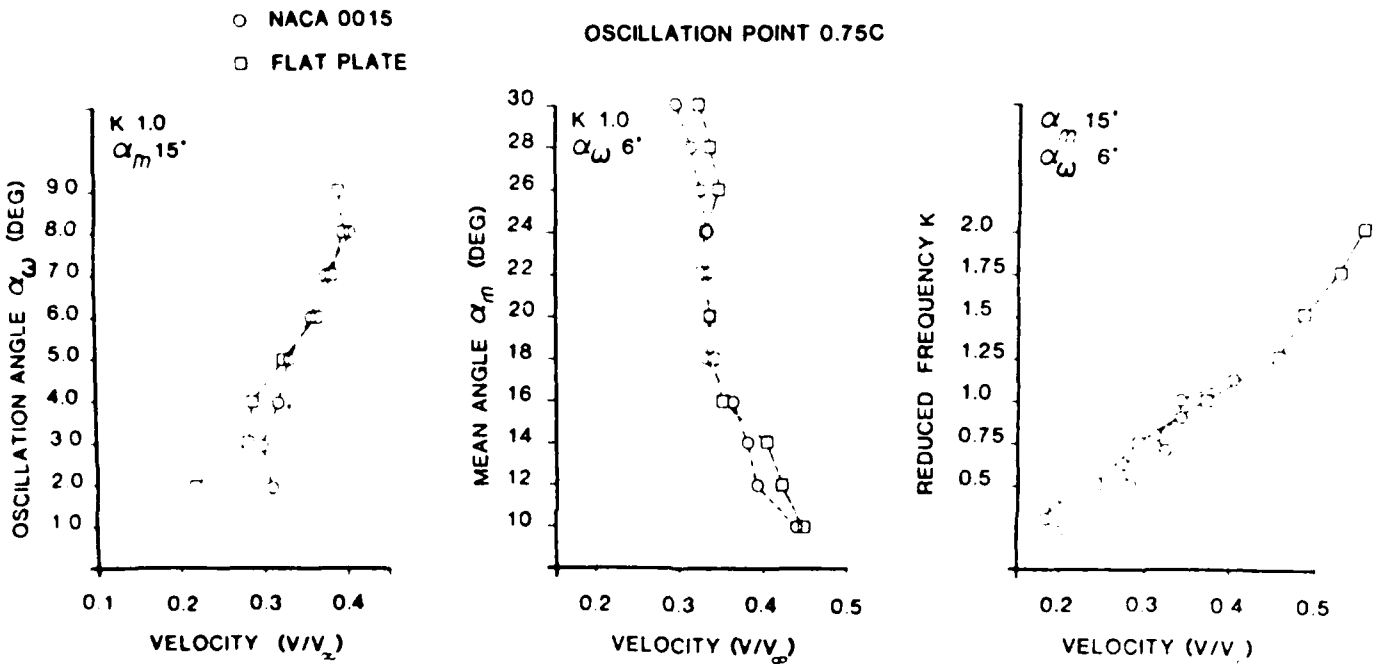

Figure 04. Comparison of α_m, α_ω and reduced frequency parameter (K) effects on the visualized convecting or traversing velocity of the leading edge vortex from 0.2 to 1.0 chord locations. The test surfaces were as noted in Fig. 02. Re number = 50,000.

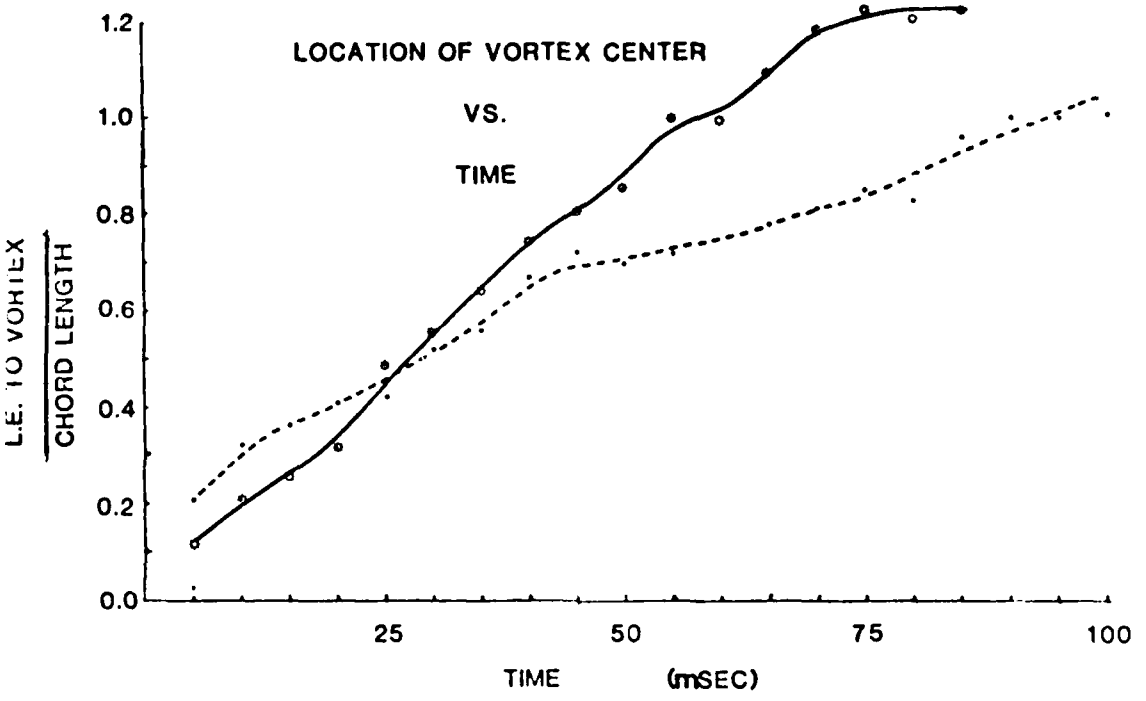

Figure 05. Flow visualization of leading edge vortex movement over the wing surface, an indication of convection velocity. The NACA 0015 airfoil fitted with curved tip was oscillated with two mean angles, α_m = 12 (solid line) and α_m = 15° (dashed line) while holding the reduced frequency at 1.0 and the α_ω at 10°. The higher α_m test resulted in a more slowly convecting vortical structure. These visualizations were done at approximately 1.0 chord inboard of the wing tip.

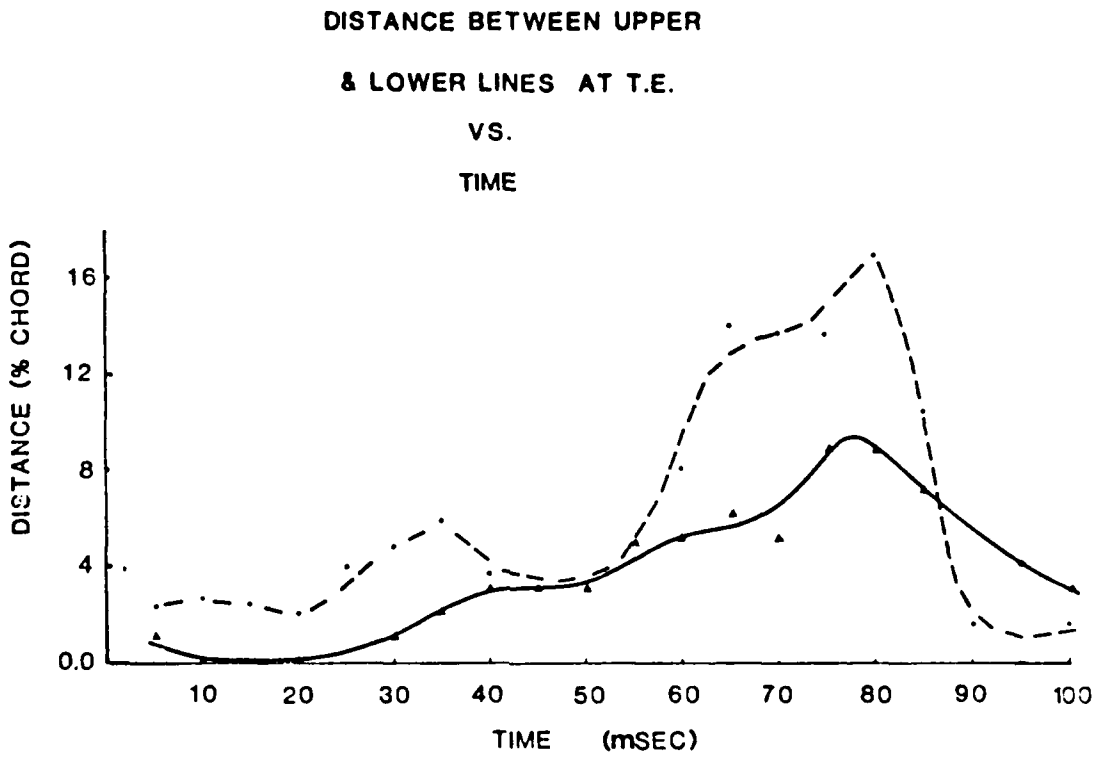

Figure 06. Displacement of upper and lower smokelines as a function of altered α_m values. The spanwise displacement of smoke passing beneath and over the wing was recorded from the time of leading edge vortex initiation to the time of leading edge passage over the trailing edge. The same test conditions as shown in Fig. 05. At 0-20 m sec, the smokelines passing the trailing edge are arranged in an unperturbed vertical stacking. At later times, coincident with the arrival and passage of the leading edge vortex, the smokelines show considerable displacement spanwise. The largest amount of displacement arises from the $\alpha_m = 15^\circ$ condition. Re ~ 60,000.

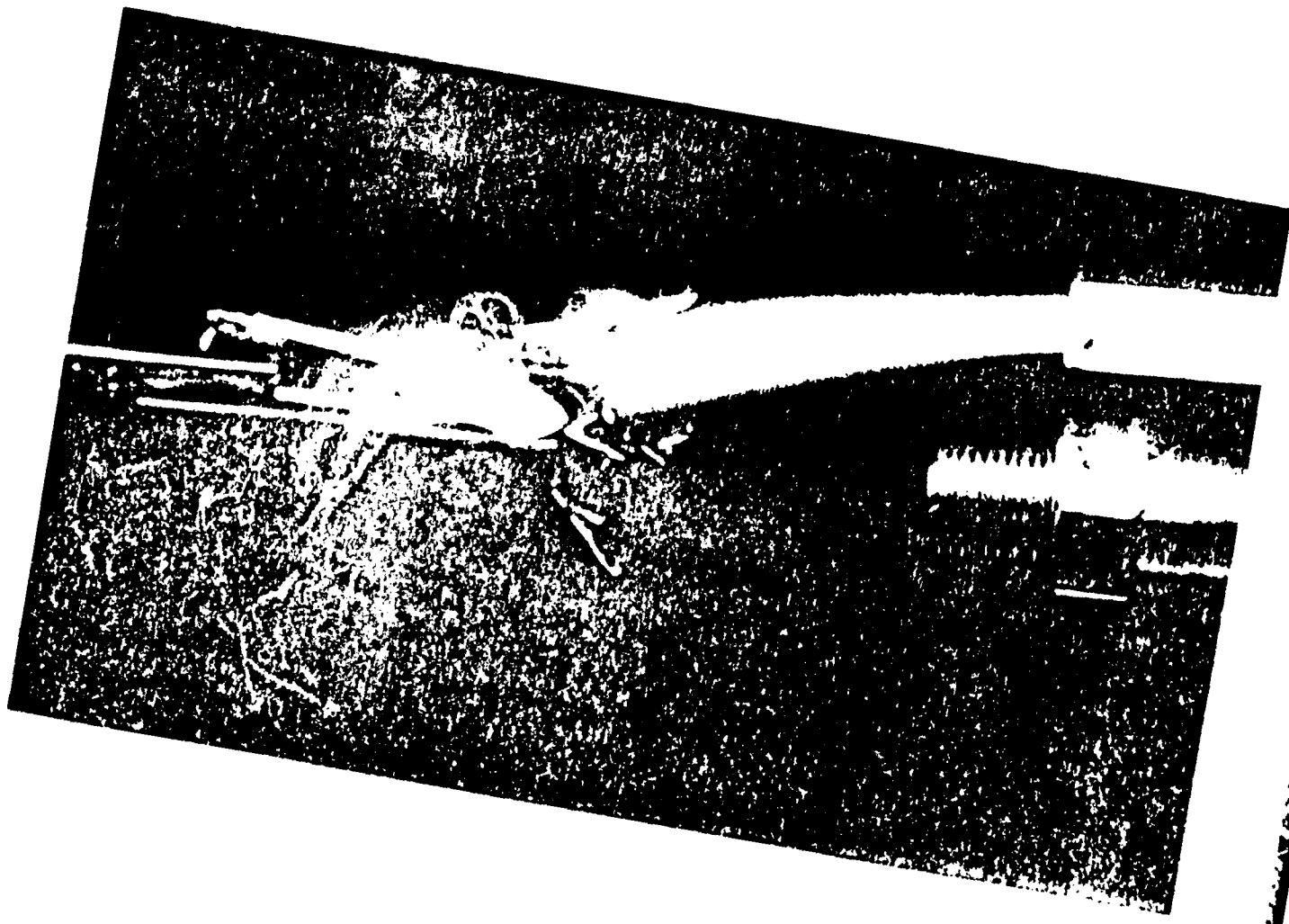

Figure 67. Flow visualization [illegible] surrounding flow. Five superimposed [illegible] exhibits small [illegible] flow structure [illegible] wings.

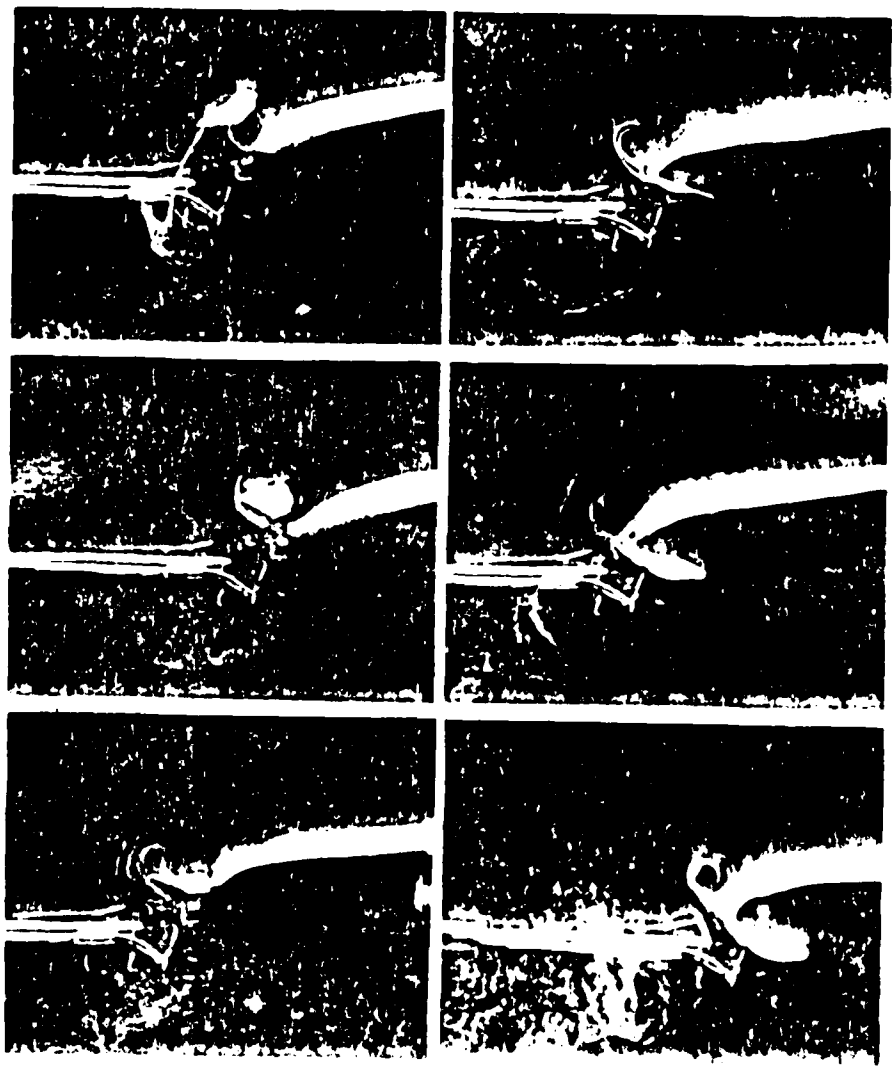

[illegible]

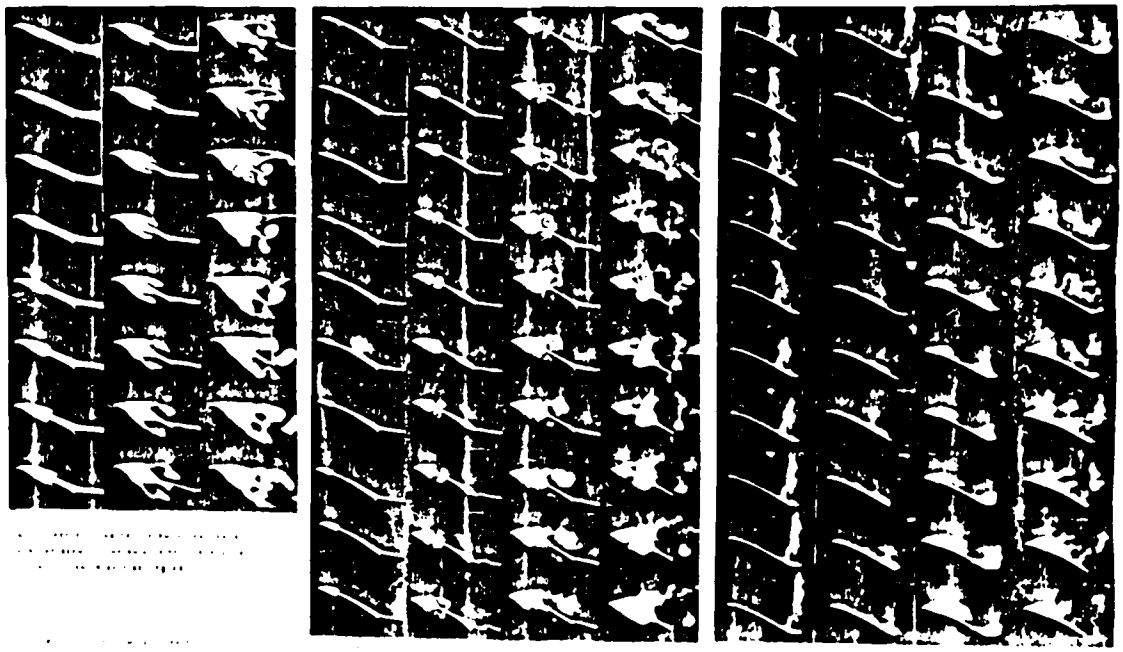

ACCELERATING FLOW OVER AN AIRFOIL. STARTING FROM REST THREE COMPLEMENTARY FLOW VISUALIZATIONS USING SMOKE

SPECIFICS NACA 0015 AIRFOIL ANGLE OF ATTACK +60° CHORD LENGTH C=15.2 + FLOW ACCELERATION A=2.4 [illegible] REYNOLDS NUMBER R=A [illegible] +5200
[illegible] KINEMATIC VISCOSITY OF AIR PHOTOGRAPHS TAKEN AT TIME T=3/4 [illegible] AFTER START FROM REST AIRFLOW FROM LEFT TO RIGHT

VISUALIZATION OF THE [illegible] FLOW USING A SMOKE WIRE COATED WITH [illegible] FOR SMOKE VISUALIZATION

IMPROVED VISUALIZATION OF THE VORTICAL FLOW BY DEPOSITING [illegible] AT THE [illegible] DOWNSTREAM FACING AIRFOIL SURFACE

THE SPIRAL STRUCTURE OF SMALL VORTICES IS REVEALED BY A [illegible] ISOGRAPH

Figure 09.

END

5-81

DTIC